Scattering of Surface Plasmon Polaritons by a Circularly Symmetric Surface Defect

A. V. Shchegrov, I. V. Novikov, and A. A. Maradudin

Department of Physics and Astronomy and Institute for Surface and Interface Science, University of California, Irvine, California 92697

(Received 3 February 1997)

By the use of the method of reduced Rayleigh equations, we develop a theory of the scattering of a surface plasmon polariton from a cirularly symmetric defect on a metal surface. We derive and solve one-dimensional integral equations for the scattering amplitudes corresponding to different rotational numbers m. We calculate the differential cross sections for scattering into the vacuum and into other surface waves, and the field intensity near the surface. The results show agreement with recent experimental data. We also consider resonant scattering due to surface shape resonances. [S0031-9007(97)03269-9]

PACS numbers: 73.20.Mf, 03.80.+r, 61.16.Ch, 61.72.Dd

A surface plasmon polariton (SPP) is a p-polarized electromagnetic wave that propagates along a vacuum-metal interface with amplitudes that decay exponentially with increasing distance into each medium from the interface. Many properties of SPP have now been studied theoretically and experimentally. Descriptions of much of this work can be found in Refs. [1] and [2].

An aspect of SPP that has been little studied up to now is their interaction with point defects on an otherwise planar metal surface, which leads to their scattering into other SPP as well as their conversion into volume electromagnetic waves in the vacuum. In a recent paper Smolyaninov *et al.* [3] have investigated the scattering of SPP by localized defects by the methods of near-field optical microscopy. In this work the authors note that at the present time there exists no theory of the scattering of a surface polariton from a single point defect on an otherwise planar metal surface. In this paper we present a nonperturbative theory of this scattering process that is based on the method of reduced Rayleigh equations [4], which is known to be exact for defects whose ratio of height to width is of the order of unity or smaller [5], and which yields accurate results for larger values of this ratio. In addition, we examine resonance effects that occur when the frequency of the SPP matches that of one of the electromagnetic surface shape resonances supported by the surface defect [6].

The physical system we study consists of vacuum in the region $x_3 > \zeta(\boldsymbol{x}_\parallel)$, where $\boldsymbol{x}_\parallel = (x_1, x_2, 0)$, and of a metal in the region $x_3 < \zeta(\boldsymbol{x}_\parallel)$. The mean free path of SPP excited by a He-Ne laser on a planar silver surface is approximately 60 μm, which is at least two orders of magnitude larger than the diameters of the defects we study. Therefore taking into account ohmic losses is not essential, and we will characterize the metal by a real frequency-dependent dielectric function $\varepsilon(\omega) < -1$. We assume that the surface profile function $\zeta(\boldsymbol{x}_\parallel)$ is a single-valued function of $\boldsymbol{x}_\parallel$, which essentially vanishes for $|\boldsymbol{x}_\parallel|$ larger than some characteristic length R. Finally, we consider a circularly symmetric $\zeta(\boldsymbol{x}_\parallel)$ that depends on $\boldsymbol{x}_\parallel$ only through its magnitude $x_\parallel$. This assumption simplifies the calculation significantly without sacrificing a great deal of generality. In this work we will use the Gaussian profile $\zeta(x_\parallel) = A\exp(-x_\parallel^2/R^2)$. The surface defect described by this function is a protuberance for $A > 0$; it is an indentation for $A < 0$.

We consider a SPP of frequency ω propagating in the x_1 direction from $x_1 = -\infty$, scattered by the surface defect. The total electric field is given by $\boldsymbol{E}(\boldsymbol{x};t) = \boldsymbol{E}(\boldsymbol{x}|\omega)e^{-i\omega t}$, where the function $\boldsymbol{E}(\boldsymbol{x}|\omega)$ in the vacuum region $x_3 > \zeta(\boldsymbol{x}_\parallel)$ has the form

$$\begin{aligned}\boldsymbol{E}(\boldsymbol{x}|\omega) = {}& \frac{c}{\omega}[i\hat{\boldsymbol{x}}_1\beta_0(k_\parallel) - \hat{\boldsymbol{x}}_3 k_\parallel]e^{ik_\parallel x_1 - \beta_0(k_\parallel)x_3} \\ &+ \int \frac{d^2q_\parallel}{(2\pi)^2}\bigg\{\frac{c}{\omega}[i\hat{\boldsymbol{q}}_\parallel\beta_0(q_\parallel) - \hat{\boldsymbol{x}}_3 q_\parallel]A_p(\boldsymbol{q}_\parallel) \\ &+ (\hat{\boldsymbol{x}}_3 \times \hat{\boldsymbol{q}}_\parallel)A_s(\boldsymbol{q}_\parallel)\bigg\}. \qquad (1)\end{aligned}$$

The first, nonintegral, term describes the field of the incident SPP. The wave vector of the incident wave $\boldsymbol{k}_\parallel = (k_\parallel, 0, 0)$ is directed along the x_1 axis, and its magnitude is $k_\parallel(\omega) = (\omega/c)\{\varepsilon(\omega)/[\varepsilon(\omega) + 1]\}^{1/2}$ [1]. The second term in Eq. (1) represents the scattered field determined by the scattering amplitudes $A_p(\boldsymbol{q}_\parallel)$ and $A_s(\boldsymbol{q}_\parallel)$ for its p- and s-polarized components, respectively. In Eq. (1), $\boldsymbol{q}_\parallel = (q_1, q_2, 0)$, a hat over a vector indicates that it is a unit vector, e.g., $\hat{\boldsymbol{q}}_\parallel = \boldsymbol{q}_\parallel/q_\parallel$, $\beta_0(q_\parallel) = [q_\parallel^2 - \omega^2/c^2]^{1/2}$ for $q_\parallel > \omega/c$ and $\beta_0(q_\parallel) = -i[\omega^2/c^2 - q_\parallel^2]^{1/2}$ for $q_\parallel < \omega/c$. We note that the function $\beta_0(k_\parallel)$ is always real since $k_\parallel(\omega) > \omega/c$.

An expression analogous to Eq. (1) can be written for $\boldsymbol{E}(\boldsymbol{x}|\omega)$ in the metal and then used together with Eq. (1) in satisfying the boundary conditions at $x_3 = \zeta(\boldsymbol{x}_\parallel)$. However, it has been shown in Ref. [4] that the field in the medium can be eliminated from the problem. The amplitudes $A_{p,s}(\boldsymbol{q}_\parallel)$ then satisfy a matrix integral equation, called the reduced Rayleigh equation,

$$f_i(p_\parallel)A_i(\boldsymbol{p}_\parallel) + \int \frac{d^2q_\parallel}{(2\pi)^2}\times \sum_{j=p,s} g_{ij}(\boldsymbol{p}_\parallel,\boldsymbol{q}_\parallel)A_j(\boldsymbol{q}_\parallel) = -g_{ip}(\boldsymbol{p}_\parallel,\boldsymbol{k}_\parallel), \quad i = p,s\,, \tag{2}$$

where

$$f_p(p_\parallel) = [\varepsilon(\omega)\beta_0(p_\parallel) + \beta(p_\parallel)]/[1-\varepsilon(\omega)],$$

$$f_s(p_\parallel) = [\beta_0(p_\parallel) + \beta(p_\parallel)]/[1-\varepsilon(\omega)],$$

$$g_{pp}(\boldsymbol{p}_\parallel,\boldsymbol{q}_\parallel) = J(\boldsymbol{p}_\parallel,\boldsymbol{q}_\parallel)[p_\parallel q_\parallel - \beta(p_\parallel)\beta_0(q_\parallel)\hat{\boldsymbol{p}}_\parallel\cdot\hat{\boldsymbol{q}}_\parallel],$$

$$g_{ps}(\boldsymbol{p}_\parallel,\boldsymbol{q}_\parallel) = -J(\boldsymbol{p}_\parallel,\boldsymbol{q}_\parallel)(i\omega/c)\beta(p_\parallel)(\hat{\boldsymbol{p}}_\parallel\times\hat{\boldsymbol{q}}_\parallel)_3\,,$$

$$g_{sp}(\boldsymbol{p}_\parallel,\boldsymbol{q}_\parallel) = J(\boldsymbol{p}_\parallel,\boldsymbol{q}_\parallel)(i\omega/c)\beta_0(q_\parallel)(\hat{\boldsymbol{p}}_\parallel\times\hat{\boldsymbol{q}}_\parallel)_3\,,$$

$$g_{ss}(\boldsymbol{p}_\parallel,\boldsymbol{q}_\parallel) = J(\boldsymbol{p}_\parallel,\boldsymbol{q}_\parallel)(\omega^2/c^2)\hat{\boldsymbol{p}}_\parallel\cdot\hat{\boldsymbol{q}}_\parallel\,,$$

$$J(\boldsymbol{p}_\parallel,\boldsymbol{q}_\parallel) = \frac{1}{\beta(p_\parallel)-\beta_0(q_\parallel)} \times \int d^2x_\parallel\, e^{-i(\boldsymbol{p}_\parallel-\boldsymbol{q}_\parallel)\cdot\boldsymbol{x}_\parallel} \times [e^{[\beta(p_\parallel)-\beta_0(q_\parallel)]\zeta(\boldsymbol{x}_\parallel)} - 1],$$

and $\beta(q_\parallel) = [q_\parallel^2 - \varepsilon(\omega)\omega^2/c^2]^{1/2}$. Within the Rayleigh hypothesis, Eq. (2) is the exact equation for the scattering amplitudes $A_{p,s}(\boldsymbol{q}_\parallel)$ for an arbitrary surface profile. From this point we will exploit the circular symmetry of $\zeta(x_\parallel)$. We factor out the dependence on the azimuthal angle $\varphi_q = \tan^{-1}(q_2/q_1)$ by means of the expansion

$$A_{p,s}(\boldsymbol{q}_\parallel) = \frac{b_{p,s}^{(0)}(q_\parallel)}{2} + \sum_{m=1}^{\infty}[b_{p,s}^{(m)}(q_\parallel)\cos(m\varphi_q) + c_{p,s}^{(m)}(q_\parallel)\sin(m\varphi_q)], \tag{3}$$

After substitution of Eq. (3) into Eq. (2) the equations for different m's decouple, reducing the problem to solving one-dimensional integral equations. The amplitudes $\{b_s^{(m)}(q_\parallel), c_p^{(m)}(q_\parallel)\}$ satisfy a pair of homogeneous equations and, therefore, vanish. This simplification occurs due to the fact that the incident field is an even function of x_2. The functions $\{b_p^{(m)}(q_\parallel), c_s^{(m)}(q_\parallel)\}$ satisfy the pair of integral equations

$$f_p(p_\parallel)b_p^{(m)}(p_\parallel) + \int_0^\infty \frac{dq_\parallel}{2\pi}\, q_\parallel[h_{pp}^{(m)}(p_\parallel,q_\parallel)b_p^{(m)}(q_\parallel) + h_{ps}^{(m)}(p_\parallel,q_\parallel)c_s^{(m)}(q_\parallel)] = -2h_{pp}^{(m)}(p_\parallel,k_\parallel)\,, \tag{4a}$$

$$f_s(p_\parallel)c_s^{(m)}(p_\parallel) + \int_0^\infty \frac{dq_\parallel}{2\pi}\, q_\parallel[h_{sp}^{(m)}(p_\parallel,q_\parallel)b_p^{(m)}(q_\parallel) + h_{ss}^{(m)}(p_\parallel,q_\parallel)c_s^{(m)}(q_\parallel)] = -2h_{sp}^{(m)}(p_\parallel,k_\parallel)\,. \tag{4b}$$

We note that a single integral equation for $b_p^{(0)}(q_\parallel)$ is obtained by setting $c_s^{(0)}(q_\parallel) \equiv 0$ in Eq. (4a). In Eqs. (4a) and (4b) we have used the notations

$$h_{pp}^{(m)}(p_\parallel,q_\parallel) = p_\parallel q_\parallel N_m - \frac{1}{2}\beta(p_\parallel)\beta_0(q_\parallel)[N_{m-1}+N_{m+1}],$$

$$h_{ps}^{(m)}(p_\parallel,q_\parallel) = -(i\omega/2c)\beta(p_\parallel)[N_{m-1}-N_{m+1}],$$

$$h_{sp}^{(m)}(p_\parallel,q_\parallel) = -(i\omega/2c)\beta_0(q_\parallel)[N_{m-1}-N_{m+1}],$$

$$h_{ss}^{(m)}(p_\parallel,q_\parallel) = (\omega^2/2c^2)[N_{m-1}+N_{m+1}],$$

Here N_m stands for the function

$$N_m(p_\parallel,q_\parallel) = \frac{2\pi}{\beta(p_\parallel)-\beta_0(q_\parallel)} \times \int_0^\infty dx_\parallel\, x_\parallel[e^{(\beta(p_\parallel)-\beta_0(q_\parallel))\zeta(x_\parallel)} - 1] \times J_m(p_\parallel x_\parallel)J_m(q_\parallel x_\parallel)\,, \tag{5}$$

where $J_m(z)$ is a Bessel function. For the Gaussian surface $\zeta(x_\parallel) = A\exp(-x_\parallel^2/R^2)$, which we consider in this work, N_m can be represented in a form of a rapidly converging series [6].

Since the unperturbed system (without the defect) supports surface excitations of p polarization, the scattering amplitude $A_p(\boldsymbol{q}_\parallel)$ and, hence, $\{b_p^{(m)}(q_\parallel)\}$, must have a pole at $q_\parallel = k_\parallel(\omega) + i\eta$, where the positive imaginary infinitesimal $i\eta$ is added to ensure that the scattered surface waves are outgoing. Therefore, in solving Eqs. (4) we will seek the functions $\{b_p^{(m)}(q_\parallel)\}$ in the form

$$b_p^{(m)}(q_\parallel) = \tilde{b}_p^{(m)}(q_\parallel)/f_p(q_\parallel)\,, \tag{6}$$

where $\{\tilde{b}_p^{(m)}(q_\parallel)\}$ are nonsingular, and the denominator $f_p(q_\parallel)$ vanishes at $q_\parallel = k_\parallel(\omega)$. In substituting Eq. (6) into Eqs. (4), we use the identity $1/f_p(q_\parallel) = P[1/f_p(q_\parallel)] + \{i\pi\beta(k_\parallel)/k_\parallel[\varepsilon(\omega)+1]\}\delta(q_\parallel - k_\parallel)$.

We solve the resulting equations for $\{\tilde{b}_p^{(m)}(q_\parallel), c_s^{(m)}(q_\parallel)\}$ numerically by discretizing the range of integration and transforming the integral equations into matrix equations thereby [6]. After computing $A_{p,s}(\boldsymbol{q}_\parallel)$ in Eq. (1) using Eqs. (3) and (6), we apply the technique described in Ref. [7] to calculate the scattered field in the far zone. If $\boldsymbol{x} = x(\sin\theta_x\cos\varphi_x, \sin\theta_x\sin\varphi_x, \cos\theta_x)$ is the observation point in the vacuum, then the far field scattered away from the surface is given by the outgoing spherical wave

$$\boldsymbol{E}_{\mathrm{vac}}^{(\mathrm{sc})}(\boldsymbol{x}|\omega) = -\frac{i\omega\cos\theta_x}{2\pi c}\, e^{i(\omega/c)x}\left\{\hat{\boldsymbol{e}}_{\boldsymbol{p}} A_p\left(\hat{\boldsymbol{x}}\,\frac{\omega}{c}\sin\theta_x\right) + \hat{\boldsymbol{e}}_{\boldsymbol{s}} A_s\left(\hat{\boldsymbol{x}}\,\frac{\omega}{c}\sin\theta_x\right)\right\}, \qquad (\omega/c)x \gg 1\,, \tag{7}$$

where $\hat{\boldsymbol{e}}_{\boldsymbol{p}} = (\cos\theta_x\cos\varphi_x, \cos\theta_x\sin\varphi_x, -\sin\theta_x)$, and $\hat{\boldsymbol{e}}_{\boldsymbol{s}} = (-\sin\varphi_x, \cos\varphi_x, 0)$ are polarization vectors. The far field scattered into other surface waves measured at $\boldsymbol{x}_\parallel = x_\parallel(\cos\varphi_x, \sin\varphi_x, 0)$ has the form of an outgoing cylindrical wave,

$$\boldsymbol{E}_{\mathrm{SPP}}^{(\mathrm{sc})}(\boldsymbol{x}|\omega) = \frac{e^{ik_\parallel x_\parallel + i(\pi/4) - \beta_0(k_\parallel)x_3}}{(2\pi k_\parallel x_\parallel)^{1/2}}\,\frac{c\beta(k_\parallel)}{\omega} \times \frac{[i\hat{\boldsymbol{x}}_\parallel\beta_0(k_\parallel) - \hat{\boldsymbol{x}}_3 k_\parallel]}{\varepsilon(\omega) + 1}\,\tilde{A}_p(\hat{\boldsymbol{x}}_\parallel k_\parallel)\,, \quad k_\parallel x_\parallel \gg 1\,, \tag{8}$$

where $\tilde{A}_p(\boldsymbol{q}_\parallel) = \tilde{b}_p^{(0)}(q_\parallel)/2 + \sum_{m=1}^{\infty}\tilde{b}_p^{(m)}(q_\parallel)\cos(m\varphi_q)$. We define the differential cross sections, measured in units of length, for scattering into the vacuum and into other surface waves as

$$\sigma_{\mathrm{vac}}(\theta_x, \varphi_x) = \frac{P_{\mathrm{vac}}(\theta_x, \varphi_x)}{P_{\mathrm{inc}}}\,, \qquad \sigma_{\mathrm{SPP}}(\varphi_x) = \frac{P_{\mathrm{SPP}}(\varphi_x)}{P_{\mathrm{inc}}}\,, \tag{9}$$

where $P_{\mathrm{vac}}(\theta_x, \varphi_x)$ is the power scattered into the vacuum away from the surface in the direction $\hat{\boldsymbol{x}}$, $P_{\mathrm{SPP}}(\varphi_x)$ is the power scattered into the surface waves in the direction $\hat{\boldsymbol{x}}_\parallel$, and P_{inc} is the incident power per unit length in the x_2 direction.

We present numerical results for a Gaussian indentation characterized by $A = -0.05\ \mu$m and $R = 0.25\ \mu$m on a silver surface with $\varepsilon(\omega) = -17.8$, which parameters correspond approximately to one of the cases considered experimentally [3]. This value of $\varepsilon(\omega)$ corresponds to the wavelength in vacuum $\lambda = 0.6328\ \mu$m for the He-Ne laser.

In Fig. 1 we present a contour plot of $\sigma_{\mathrm{vac}}(\theta_x, \varphi_x)$. The maximum of the scattering intensity occurs at $\theta_x = 28°$, $\varphi_x = 0°$. The total cross section for the waves radiated into the vacuum, $\sigma_{\mathrm{vac}}^{(\mathrm{tot})}$ in this case is only $3.7 \times 10^{-3}\ \mu$m, which is not a surprising result for such a shallow defect. The result for $\sigma_{\mathrm{vac}}^{(\mathrm{tot})}$ is of the same order of magnitude as $\sigma_{\mathrm{SPP}}^{(\mathrm{tot})} = 2.6 \times 10^{-3}\ \mu$m. The angular dependence of $\sigma_{\mathrm{SPP}}(\varphi_x)$ is shown in Fig. 2. We see that the scattering of SPP in the forward and backward directions is suppressed. The main portion of the scattered energy goes into two SPP beams separated by approximately 70°. This result is even better illustrated by Fig. 3, which shows the field intensity $|\boldsymbol{E}(\boldsymbol{x}|\omega)|^2$ at 5 nm above the surface profile $[x_3 = \zeta(x_\parallel) + 5\ \mathrm{nm}]$, which corresponds to the quantity measured in Ref. [3]. Both Figs. 2 and 3 confirm the experimental data [3], especially the shadow behind the defect [see Fig. 3(b) of Ref. [3]]. Although the authors of Ref. [3] mentioned that these rather large "angle values cannot be accounted for by diffraction," we believe that they can be. Since it is difficult to understand the origin of this phenomenon from the exact calculation, we invoke the first Born approximation which corresponds to neglecting the integral term on the left-hand side of Eq. (2) and keeping only the linear term in the profile's amplitude on the right-hand side. Although $k_\parallel|A| \cong 0.53$ for the defect we consider, this approximation should give the leading contribution to $\sigma_{\mathrm{SPP}}(\varphi_x)$:

$$\sigma_{\mathrm{SPP}}^{\mathrm{Born}}(\varphi_x) \cong 2\pi R(A/R)^2(k_\parallel R)^5\{|\varepsilon(\omega)|/[\varepsilon(\omega) + 1]^2\} \times \sin^4(\varphi_x/2)\exp[-2k_\parallel^2 R^2\sin^2(\varphi_x/2)]\,. \tag{10}$$

We have compared results of exact numerical calculations with those obtained on the basis of Eq. (10), and find that $\sigma_{\mathrm{SPP}}(\varphi_x)$ is very well approximated by $\sigma_{\mathrm{SPP}}^{\mathrm{Born}}(\varphi_x)$ for $k_\parallel|A| \ll 1$ and $\varepsilon(\omega)$ not close to -1, when $\sigma_{\mathrm{SPP}}^{\mathrm{Born}}(\varphi_x)$ diverges. Scattering in the forward direction is absent in

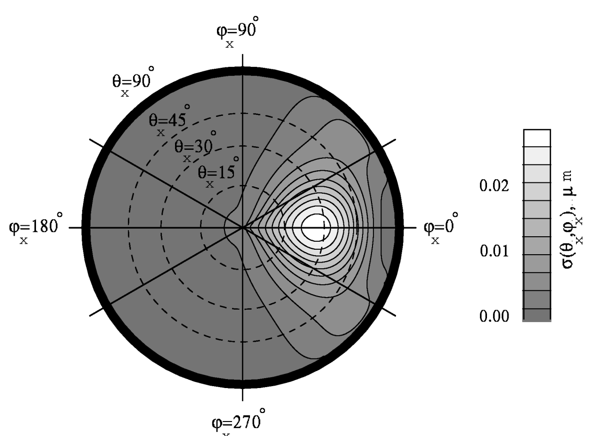

FIG. 1. A contour plot of $\sigma_{\mathrm{vac}}(\theta_x, \varphi_x)$. The concentric circles are the lines of constant θ_x, with $\theta_x = 0°$ in the center, $\theta_x = 90°$ at the border. The azimuthal angle φ_x varies from 0° to 360°. $A = -0.05\ \mu$m and $R = 0.25\ \mu$m.

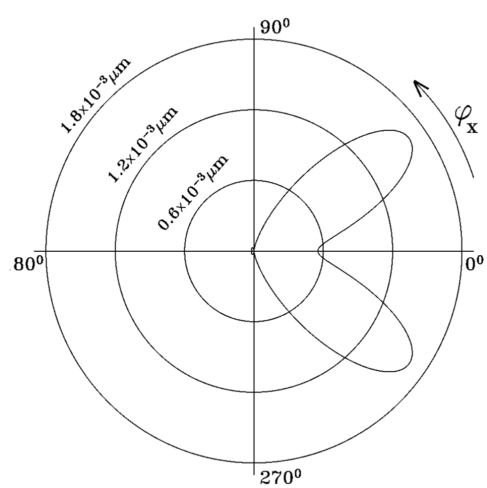

FIG. 2. A polar plot of $\sigma_{\mathrm{SPP}}(\varphi_x)$ for $A = -0.05\ \mu$m and $R = 0.25\ \mu$m.

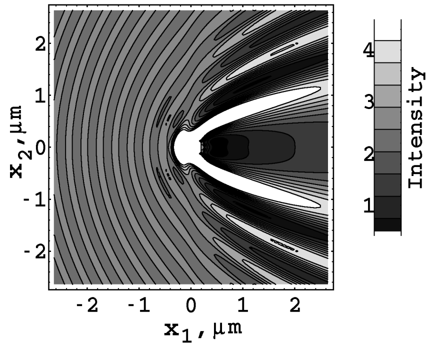

FIG. 3. The field intensity $|\boldsymbol{E}(\boldsymbol{x}|\omega)|^2$ as a function of $\boldsymbol{x}_\parallel$ for $x_3 = \zeta(x_\parallel) + 5$ nm, $A = -0.05$ μm, and $R = 0.25$ μm.

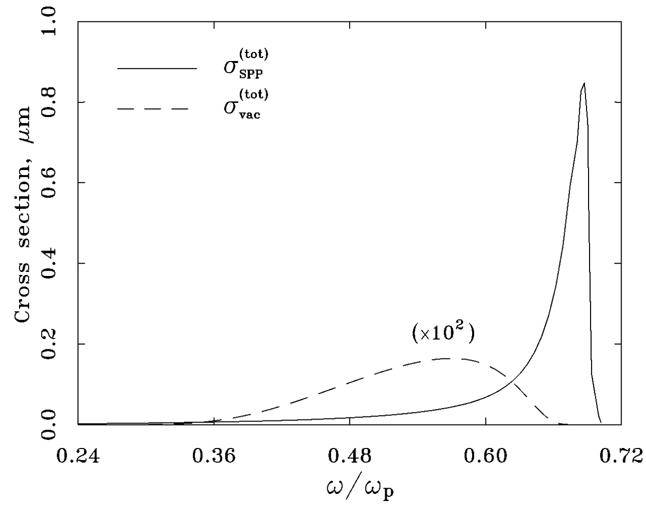

FIG. 4. The cross sections $\sigma^{(\text{tot})}_{\text{SPP}}$ and $\sigma^{(\text{tot})}_{\text{vac}}$ as functions of ω/ω_p for $A = -0.05$ μm and $R = 0.25$ μm.

the first Born approximation. If $k_\parallel R$ is small as well as $k_\parallel|A|$, then the scattering is close to isotropic (the $m = 0$ channel is dominant), and the frequency dependence ω^5 represents the Rayleigh scattering law. For $k_\parallel R > 1$ the function (10) has two maxima at $\varphi_{\max} = \pm 2\sin(1/k_\parallel R)$. For example, for the defect we consider $k_\parallel R \cong 2.63$, which would give an angular separation of 88° for the maxima if the condition $k_\parallel|A| \ll 1$ were well satisfied. Thus, large diffraction angles even for small defects are not surprising. Smolyaninov *et al.* [3] also point out that the shadow source appears to be too large for the actual size of the scatterer, suggesting quite a large value for the cross section. We believe that this is not so, since even the Born approximation (10) can give large diffraction angles for very small values of $\sigma^{(\text{tot})}_{\text{SPP}}$ compared to R. We also note that some features one sees in Fig. 3 (additional weaker diffraction maxima, etc.) but does not see in the experimental image are due to the fact that the tip used for measuring the intensity in Ref. [3] is not a point detector in both the vertical and lateral directions. Its actual lateral resolution is around 0.1–0.2 μm [8]. Therefore, the comparison can be performed only on average.

We conclude our analysis by considering resonant scattering of SPP. Maradudin and Visscher [6] showed that a localized surface defect supports electromagnetic surface shape resonances—excitations with a finite lifetime, which decay into volume and surface waves. The resonances with the longest lifetime were found to exist in the region of ω, in which $\varepsilon(\omega)$ is slightly smaller than -1. Assuming the free-electron model $\varepsilon(\omega) = 1 - \omega_p^2/\omega^2$, we have calculated and plotted in Fig. 4 $\sigma^{(\text{tot})}_{\text{vac}}(\omega)$ and $\sigma^{(\text{tot})}_{\text{SPP}}(\omega)$ for the same defect. We see that $\sigma^{(\text{tot})}_{\text{SPP}}(\omega)$ becomes comparable with R near $\omega = \omega_p/\sqrt{2}$, and peaks at the resonance frequency $\omega \cong 0.687\omega_p$. In contrast, $\sigma^{(\text{tot})}_{\text{vac}}$ remains small in this region of ω. This is not surprising since it was shown recently [9] that resonant states associated with surface defects do not always reveal themselves in the field scattered into the vacuum away from the surface.

In conclusion, we have developed a theory of scattering of SPP from a circularly symmetric defect on an otherwise planar metal surface. The method based on the reduced Rayleigh equations proves to be a simple, computationally feasible approach that yields nonperturbative solutions for a wide class of surface defects for which the Rayleigh hypothesis is valid. For surface profiles that can be approximated by a cylindrically symmetric function, we reduce the problem to solving one-dimensional integral equations. The results show a good agreement with recent experimental data [3]. In many experimental situations both vertical and lateral sizes of the defect are small compared to the wavelength of the incident SPP. For this case, we have derived an analytical formula (10) in the Born approximation for the cross section for scattering into other SPP. Finally, we have shown that when the frequency of the SPP matches that of one of the surface shape resonances supported by the surface defect, the cross section for the scattering of SPP into SPP is enhanced.

The authors would like to thank I. Smolyaninov for helpful discussions concerning the results presented in Ref. [3]. This research was supported in part by Army Research Office Grant No. DAAH 04–96–1–0187.

[1] *Surface Polaritons*, edited by V. M. Agranovich and D. L. Mills (North-Holland, Amsterdam, 1982).
[2] *Electromagnetic Surface Modes*, edited by A. D. Boardman (Wiley, New York, 1982).
[3] I. I. Smolyaninov, D. I. Mazzoni, and C. C. Davis, Phys. Rev. Lett. **77**, 3877 (1996).
[4] G. C. Brown, V. Celli, M. Haller, and A. Marvin, Surf. Sci. **136**, 381 (1984).
[5] P. M. van den Berg and J. T. Fokkema, Radio Sci. **15**, 723 (1980).
[6] A. A. Maradudin and W. M. Visscher, Z. Phys. B **60**, 215 (1985).
[7] D. L. Mills, Phys. Rev. B **12**, 4036 (1975).
[8] I. I. Smolyaninov (private communication).
[9] A. A. Maradudin, A. V. Shchegrov, and T. A. Leskova, Opt. Commun. **135**, 352 (1997).